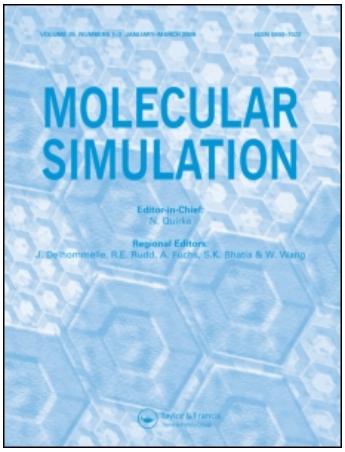

Molecular Simulation
Publication details, including instructions for authors and subscription information:
http://www.informaworld.com/smpp/title~content=t713644482

Simulation study of discotic molecules in the vicinity of the isotropic-liquid crystal transition

Bruno Martínez-Haya[a]; Alejandro Cuetos[b]
[a] Departamento de Sistemas Físicos, Químicos y Naturales, Universidad Pablo de Olavide, Seville, Spain [b] Departamento de Física Aplicada, Universidad de Almería, Almería, Spain

To cite this Article Martínez-Haya, Bruno and Cuetos, Alejandro(2009) 'Simulation study of discotic molecules in the vicinity of the isotropic-liquid crystal transition', Molecular Simulation, 35: 12, 1077 — 1083
To link to this Article: DOI: 10.1080/08927020902833111
URL: http://dx.doi.org/10.1080/08927020902833111

Molecular Simulation
Vol. 35, Nos. 12–13, October–November 2009, 1077–1083

Taylor & Francis
Taylor & Francis Group

Simulation study of discotic molecules in the vicinity of the isotropic–liquid crystal transition

Bruno Martínez-Haya[a]* and Alejandro Cuetos[b1]

[a]*Departamento de Sistemas Físicos, Químicos y Naturales, Universidad Pablo de Olavide, 41013 Seville, Spain;* [b]*Departamento de Física Aplicada, Universidad de Almería, 04020 Almería, Spain*

(*Received 8 December 2008; final version received 16 February 2009*)

The equilibrium and microscopic properties of systems of discotic molecules have been investigated with Monte Carlo (MC) simulations. The study focuses on the behaviour of the fluid in the isotropic phase in the vicinity of the first liquid crystal transition, which involves either a nematic or a columnar phase. The molecules are modelled by rigid oblate spherocylinders with various types of interaction potentials. Molecular thickness/diameter ratios within $L/D = 0.1–0.5$ are considered. The MC equations of state are compared with theoretical predictions for hard convex bodies, based on molecular shape and virial expansions. A good agreement is found for the hard spherocylinder system, although discrepancies arise for $L/D < 0.4$ at sufficiently large packing fraction. Particular efforts are also devoted to characterising the formation of domains of stacked molecules in the isotropic phase for the different repulsive and attractive interaction models.

Keywords: liquid crystals; discotic molecules; stacking; Monte Carlo; equations of state

1. Introduction

Discotic molecules are at the heart of a vast number of technological applications, ranging from liquid crystals [1,2] to nanoelectronic devices [3]. Planar disk-like molecular structures are also involved in the stacking phenomena that govern a broad class of colloidal and biochemical aggregation processes. Discotic molecules are often complex organic compounds. Remarkable efforts have been directed towards the theoretical description of stacking interactions in these systems from first principles [4], or in classical atomistic approaches [5,6]. Due to molecular complexity, atomistic studies are computationally expensive. As a consequence, the investigation of discotic fluids demands complementary approaches, based on a coarse-grain description of the molecular structure and of the relevant interactions. Ideally, such a modelling framework should still capture the physics underlying the microscopic and mesophasic behaviours of discotics. The success of coarse-grain models relies on the central role that excluded volume interactions, induced by molecular shape, play in colloidal behaviour.

Coarse-grain studies of discotic molecules have been much more scarce than those of rod-like molecules. In a recent work [7], we have introduced an efficient methodology of general application for discotics. Our approach is based on the use of Kihara-type pair potentials to represent the particles as rigid discotic spherocylinders. This particle geometry (a flat cylindrical core with a toroidal rim) is represented in Figure 1. Discotic spherocylinders can be expected to resemble more closely the effective shape of rigid discotic mesogens than, for instance, ellipsoidal models [8].

We report here on a study of discotic Kihara models with thickness/diameter ratios within $L^* \equiv L/D = 0.1–0.5$. Computational and theoretical studies for this family of molecular fluids have been restricted thus far to the hard spherocylinder fluid (OHSC). Furthermore, most previous works have been limited to the isotropic phase of particles with a moderate anisotropy ($L^* > 0.3$) [10–17]. Only very recently, a detailed account of different columnar phases displayed by the OHSC fluid has been reported from MC simulations [7]. This latter study demonstrated that the discotic spherocylinder molecular shape intrinsically favours columnar stacking, as opposed to hard discotic ellipsoids of revolution, which lack columnar phases, unless specific energetics are incorporated [8,9].

In the present study, we consider four different types of pair interaction potentials. On one hand, hard and soft repulsive spherocylinders are investigated. Furthermore, spherocylinders with soft attractive interactions around the molecular core are considered. *Ab initio* computations for planar polyaromatics have shown that pair interactions depend strongly on the relative orientation of the particles, even if the shortest distance between the molecular cores remains unchanged [4]. Correspondingly, we have incorporated attractive interactions with an explicit dependence on pair orientation into our coarse-grain model. In order to achieve this, we have followed an approach applied previously to rod-like Kihara particles [18–21].

*Corresponding author. Email: bmarhay@upo.es

ISSN 0892-7022 print/ISSN 1029-0435 online

DOI: 10.1080/08927020902833111
http://www.informaworld.com

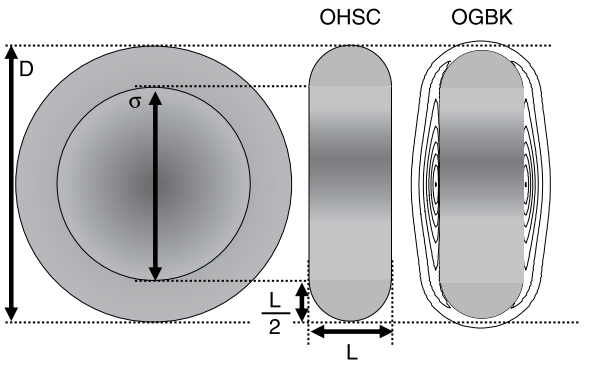

Figure 1. Representation of an oblate spherocylinder. Left: top view; right: side views for the hard OHSC model (Equation (4)) and for the soft OGKB model with orientational dependent interactions (Equation (7)).

Within this framework, it is possible to build interaction potentials resembling the features exposed by the *ab initio* computations on planar and dendritic molecular systems [4]. In particular, it allows to mimic the interactions in graphene sheets, including systems with localised active sites.

Our colleague J.A. Mejías [22,23] was intensively involved in the understanding of molecular processes on soots, a particularly important class of graphene networks with active sites. As a modest tribute to his memory, we pursue the development of coarse-grain models with specific interactions that may serve to establish effective links between statistical mechanics and quantum chemistry for such systems.

This paper focuses on the behaviour of the model discotics in the isotropic phase, beginning at the transition from the liquid crystal phase with which it coexists. After describing the interaction models in Section 2, the equations of state are presented and compared with the prediction of previous theoretical approaches. Finally, one main microscopic feature of the Kihara discotics is discussed, namely the propensity to form domains of stacked particles in the isotropic phase. Future work in our group will extend the study to determine the role of specific pair interactions on aggregation phenomena, and on the mesogenic properties of these fluids.

2. Methodology

2.1 Spherocylinder particle geometry

Figure 1 depicts the molecular shape of the discotic Kihara models. The surface of a hard discotic spherocylinder corresponds to the ensemble of points that are at a distance $L/2$ from an infinitely thin disk of diameter σ. The total diameter of the particle is then given by $D = \sigma + L$, and its thickness/diameter aspect ratio by $L^* = L/D$. Particles with greater values of L^* have a less planar, more spherical shape. The present study includes molecules with constant σ, and variable aspect ratios within $L^* = 0.1–0.5$. Note then that the increase in L^* involves an increment in the molecular volume (see Equation (1)).

We will compare the present simulation results for the equation of state (EOS) of the hard discotic spherocylinder fluid with predictions for hard convex bodies, based on molecular shape and virial expansions [24,25]. Barrio and Solana [24] proposed a scaling of the Carnahan–Starling EOS to predict the behaviour of convex bodies. A single scaling factor was used, namely the non-sphericity factor $\alpha = r_m s_m/(3v_m)$, which includes three basic parameters describing the molecular geometry: the volume (v_m), the surface area (s_m) and the mean curvature integral ($4\pi r_m$). Boublik [25] developed a third-order virial expansion including a more involved combination of the same parameters. For hard oblate spherocylinders, these geometric parameters are given by the following expressions [11]:

$$v_m/D^3 = \frac{\pi L^{*3}}{6} + \frac{\pi^2(1-L^*)L^{*2}}{8} + \frac{\pi(1-L^*)^2 L^*}{4}, \quad (1)$$

$$s_m/D^2 = \pi L^{*2} + \frac{\pi^2(1-L^*)L^*}{2} + \frac{\pi(1-L^*)^2}{2}, \quad (2)$$

$$r_m/D = \frac{L^*}{2} + \frac{\pi(1-L^*)}{8}. \quad (3)$$

2.2 Pair interaction models

We will consider four types of discotic interaction models, namely the oblate versions of the OHSC model, the soft repulsive spherocylinder model (OSRS), the 12-6 Kihara model (OKIH) and the recently introduced Gay–Berne–Kihara model (OGBK) [20,21]. This latter model incorporates an explicit dependence of the dispersive interactions on pair orientation, as shown in Figure 1 and described below. For spherocylinder particles, the pair interaction energy is directly related to the shortest distance between the central disks of the molecular cores, $d_m(\mathbf{r_{ij}},\hat{\mathbf{u}}_\mathbf{i},\hat{\mathbf{u}}_\mathbf{j})$. Such distance is a complex (not analytical) function of the centre-of-mass intermolecular distance vector $\mathbf{r_{ij}}$, and of the relative orientations of the pair of particles, defined by the directors ($\hat{\mathbf{u}}_\mathbf{i}$, $\hat{\mathbf{u}}_\mathbf{j}$). A general description of the numerical algorithm employed to compute d_m can be found in [7].

The above-mentioned interaction models are defined by the following expressions.

OHSC potential:

$$U_{OHSC}(d_m) = \begin{cases} \infty & d_m \le L \\ 0 & d_m > L \end{cases} \quad (4)$$

OKIH potential:

$$U_{OKIH}(d_m) = 4\varepsilon\left[(L/d_m)^{12} - (L/d_m)^6\right]. \quad (5)$$

OSRS potential:

$$U_{\mathrm{OSRS}}(d_{\mathrm{m}}) = \begin{cases} 4\varepsilon\left[\left(L/d_{\mathrm{m}}\right)^{12} - \left(L/d_{\mathrm{m}}\right)^{6} + 1/4\right] & d_{\mathrm{m}} \le \sqrt[6]{2}L \\ 0 & d_{\mathrm{m}} > \sqrt[6]{2}L \end{cases} \tag{6}$$

OGBK potential:

$$U_{\mathrm{OGBK}}(\mathbf{r_{ij}}, \hat{\mathbf{u}}_{\mathbf{i}}, \hat{\mathbf{u}}_{\mathbf{j}}) = \varepsilon_{\mathrm{OGB}}(\hat{\mathbf{r}}_{\mathbf{ij}}, \hat{\mathbf{u}}_{\mathbf{i}}, \hat{\mathbf{u}}_{\mathbf{j}}) U_{\mathrm{OKIH}}(d_{\mathrm{m}}), \tag{7}$$

$$\varepsilon_{\mathrm{OGB}}(\hat{\mathbf{r}}_{\mathbf{ij}}, \hat{\mathbf{u}}_{\mathbf{i}}, \hat{\mathbf{u}}_{\mathbf{j}}) = \varepsilon_{\mathrm{GO}}^{\nu}(\hat{\mathbf{u}}_{\mathbf{i}}, \hat{\mathbf{u}}_{\mathbf{j}}) \varepsilon'^{\mu}(\hat{\mathbf{r}}_{\mathbf{ij}}, \hat{\mathbf{u}}_{\mathbf{i}}, \hat{\mathbf{u}}_{\mathbf{j}}), \tag{8}$$

$$\varepsilon_{\mathrm{GO}}(\hat{\mathbf{u}}_{\mathbf{i}}, \hat{\mathbf{u}}_{\mathbf{j}}) = [1 - \chi^2 (\hat{\mathbf{u}}_{\mathbf{i}} \cdot \hat{\mathbf{u}}_{\mathbf{j}})^2]^{-1/2}, \tag{9}$$

$$\varepsilon'(\hat{\mathbf{r}}_{\mathbf{ij}}, \hat{\mathbf{u}}_{\mathbf{i}}, \hat{\mathbf{u}}_{\mathbf{j}}) = 1 - \frac{\chi'}{2}\left[\frac{(\hat{\mathbf{r}}_{\mathbf{ij}} \cdot \hat{\mathbf{u}}_{\mathbf{i}} + \hat{\mathbf{r}}_{\mathbf{ij}} \cdot \hat{\mathbf{u}}_{\mathbf{j}})^2}{1 + \chi' \hat{\mathbf{u}}_{\mathbf{i}} \cdot \hat{\mathbf{u}}_{\mathbf{j}}} + \frac{(\hat{\mathbf{r}}_{\mathbf{ij}} \cdot \hat{\mathbf{u}}_{\mathbf{i}} - \hat{\mathbf{r}}_{\mathbf{ij}} \cdot \hat{\mathbf{u}}_{\mathbf{j}})^2}{1 - \chi' \hat{\mathbf{u}}_{\mathbf{i}} \cdot \hat{\mathbf{u}}_{\mathbf{j}}}\right]. \tag{10}$$

It can be noted that the OSRS interaction potential follows from the upward shift (by the well depth ε) of the OKIH potential and its truncation at the well minimum $d_{\min} = \sqrt[6]{2}L$. In this way, a continuous and derivable purely repulsive interaction potential energy functional is obtained. The OGBK interaction energy functional is built by multiplying the OKIH potential by the orientational pre-factor of the discotic Gay–Berne potential [8]. The OKIH and OGBK potentials were truncated at $d_{\mathrm{m}} = 3L$, and shifted as to make the potential continuous.

Note that the Gay–Berne factor, $\varepsilon_{\mathrm{OGB}}$ is characterised by the aspect ratio L^* (often denoted κ) and the three parameters (κ', ν, μ), with the notation $\chi = (L^{*2} - 1)/(L^{*2} + 1)$ and $\chi' = (\kappa'^{-1/\mu} - 1)/(\kappa'^{-1/\mu} + 1)$. The choice of κ', ν and μ is not straightforward, especially when comparing with real systems. In this context, interaction energies obtained from *ab initio* computational approaches become particularly useful. For the present study, we have employed the set of parameters $\kappa' = 5$, $\nu = 2$ and $\mu = 1$, as it provided a reasonable representation of the *ab initio* data of Zhao and Truhlar [4] for pericondensed polyaromatics. As illustrated by the contour plot of Figure 1, this parametrisation provides favourable energetics for stacking. For instance, for a pair of parallel particles, $\varepsilon_{\mathrm{OGB}}$ is $\kappa'^{1/\mu} = 5$ times greater for a stacked configuration than for particles with rim-to-rim contact.

2.3 MC method

Isothermal–isobaric ensemble MC (NPT-MC) simulations were carried out following the procedure described in [7]. For each value of L^*, the system was initially equilibrated in a state within the interdigitated hexatic columnar phase [7]. The fluid was subsequently melted through the different columnar and, possibly, nematic phases, to the isotropic phase. For the soft models, equilibration typically involved 2×10^5 MC cycles (up to 5×10^5 for the boundary states of the transitions), while ensemble averages scoped over 5×10^4 cycles. For the OHSC model, which is faster to run than the soft models, 10^6 and 10^5 cycles were applied for equilibration and averaging, respectively. The size of the systems (number of particles) used in the simulation for each model is indicated in Table 1.

The melting of the OHSC fluid was induced by the reduction of the pressure/temperature ratio $P^* = PD^3/k_{\mathrm{B}}T$ (where k_{B} denotes the Boltzmann constant). For the soft interaction models, OSRS, OKIH and OGBK, the melting of the liquid crystal was actually performed by increasing the temperature $T^\dagger = k_{\mathrm{B}}T/\varepsilon$, at constant pressure $P^\dagger = PD^3/\varepsilon = 100$ (note that $P^* = P^\dagger/T^\dagger$). The phase transitions were characterised by discontinuities in density, energy, bond order and nematic-order parameters, and by monitoring specific pair correlation functions [7].

A detailed account of the nematic and columnar phases displayed by the different soft models will be provided elsewhere. Here, we concentrate mainly on characterising the isotropic phase with a limited analysis of the liquid crystalline behaviour. Nevertheless, the average nematic-order parameters at the different transitions are provided in Table 1. The nematic phase can be easily discerned from any of the columnar phases from the lack of correlations in the distribution function along the directions parallel and perpendicular to the nematic director.

3. Results

Figures 2 and 3 show the MC equations of state of the OHSC fluids with the five aspect ratios considered in our study. These figures depict the isotropic branch of the fluid, from the boundary state, where the transition from a liquid crystal phase takes place. Table 1 lists relevant parameters of the boundary states at each of the transitions and indicates the type of liquid crystal phase involved. For the OHSC fluid, the transition occurs from a nematic phase (N) for $L^* = 0.1$, and from three columnar phases, namely D_{hi} for $L^* = 0.5$, D_{ho} for $L^* = 0.4$ and D_{hd} for $L^* = 0.3$ and 0.2. Here, D_{hi} denotes a hexatic interdigitated columnar phase, D_{ho} a hexatic ordered columnar phase and D_{hd} a hexatic disordered columnar phase, in which the columns become fluid-like [7]. Hence, the internal order of the lowest columnar phase is reduced as the molecular anisotropy is enhanced (i.e. L^* becomes smaller), until the nematic phase eventually becomes stable for $L^* = 0.1$. It is interesting to notice that the columnar transition shifts to smaller packing fractions as the molecules become thinner, and that the nematic transition for $L^* = 0.1$ occurs at a relatively small packing fraction of the fluid.

Table 1. Boundary states for the isotropic–liquid crystal transitions of the model fluids studied in this work.

		Isotropic phase					Liquid crystal phase					
Model fluid	N_p	P^*	η	ρ^*	U^*	S_2	P^*	η	ρ^*	U^*	S_2	Phase type
OHSC $L^* = 0.1$	3840	31	0.305(2)	3.87(3)	–	0.03(1)	32	0.291(2)	4.07(3)	–	0.499(5)	N
OHSC $L^* = 0.2$	2016	49	0.475(1)	3.29(1)	–	0.04(1)	50	0.544(1)	3.77(2)	–	0.901(4)	D_{hd}
OHSC $L^* = 0.3$	2016	45	0.514(2)	2.48(1)	–	0.03(1)	46	0.577(3)	2.78(3)	–	0.842(8)	D_{hd}
OHSC $L^* = 0.4$	3024	42	0.541(2)	2.04(1)	–	0.04(1)	43	0.602(1)	2.27(2)	–	0.853(3)	D_{ho}
OHSC $L^* = 0.5$	1680	40	0.561(1)	1.77(1)	–	0.02(1)	41	0.611(2)	1.92(2)	–	0.852(5)	D_{ii}
OSRS $L^* = 0.2$	3000	50.0	0.490(1)	3.40(1)	1.39(3)	0.04(1)	51.3	0.548(2)	3.80(1)	1.31(3)	0.856(5)	D_{hd}
OSRS $L^* = 0.4$	3024	45.5	0.576(1)	2.17(1)	3.31(5)	0.02(1)	46.5	0.634(1)	2.39(1)	3.05(5)	0.842(4)	D_{ho}
OKIH $L^* = 0.2$	3000	46.5	0.503(1)	3.49(1)	−2.47(4)	0.03(1)	47.6	0.584(2)	4.05(1)	−2.85(4)	0.879(5)	D_{hd}
OKIH $L^* = 0.4$	3024	38.5	0.576(1)	2.17(1)	−1.79(5)	0.02(1)	39.2	0.638(2)	2.41(1)	−2.56(6)	0.820(6)	D_{ho}
OGBK $L^* = 0.2$	3000	12.7	0.339(2)	2.35(1)	−9.0(1)	0.03(1)	12.8	0.519(4)	3.60(3)	−37.0(6)	0.955(2)	D_{hd}
OGBK $L^* = 0.4$	3024	21.5	0.507(1)	1.91(1)	−6.6(1)	0.02(1)	21.7	0.558(2)	2.11(1)	−13.6(2)	0.84(1)	D_{ho}

N_p, $P^* = PD^3/k_BT$, $\eta = \rho v_m$, $\rho^* = \rho D^3$, $U^* = U/\varepsilon$ and S_2 represent number of particles in the simulation, pressure/temperature ratio, packing fraction, number density, energy per particle in reduced units and nematic-order parameter, respectively. The packing fraction is given for comparison with previous studies of the OHSC fluid and is computed with the molecular volume (v_m) of an OHSC particle for each given L^* [7]. The values in brackets denote the statistical uncertainty (one SD) in the last digit. The last column indicates the type of liquid crystalline phase associated to the transition [7]. For the soft interaction models (OSRS, OKIH and OGBK), the simulations were performed at constant pressure $P^\dagger = PD^3/\varepsilon = 100$. The transition temperatures are thus given by $T^\dagger = k_BT/\varepsilon = P^\dagger/P^*$.

Figure 2. Equations of state in the isotropic phase (I) for OHSC fluids with thickness/diameter aspect ratios $L^* = 0.1$–0.5. The reduced pressure $P^* = PD^3/k_BT$ is represented against the packing fraction of the fluid η. Symbols denote MC simulation data. Lines represent the theoretical predictions of Barrio and Solana [24] and Boublik [25]. For $L^* = 0.1$, the simulation results for the nematic branch (N) are also shown (open symbols).

Two different representations of the EOS are shown in Figures 2 and 3 in order to provide a direct comparison with the analogous results for the soft particles discussed below. On one hand, the EOS is shown confronting the reduced pressure P^* with the packing fraction of the fluid, $\eta = \rho v_m$. On the other hand, the compressibility factor, $Z = \beta P/\rho = P^*/\rho^*$ is plotted against the reduced number density $\rho^* = \rho D^3$. In both representations, the EOS predicted for the OHSC fluid by the theories of [24,25] are shown for comparison. Simulation data obtained for the nematic phase of the $L^* = 0.1$ OHSC fluid are also included in Figure 2 for reference. It can be noted that the maximum packing fraction achieved by the fluid in the isotropic phase increases with growing L^*. This follows

Figure 3. Compressibility factor $Z = P^*/\rho^*$ versus reduced density $\rho^* = \rho D^3$ representation of the same isotropic phase equations of state shown in Figure 1.

from the greater excluded volume induced by the thinner particles, in comparison with their molecular volume, under conditions of random orientation. Similar considerations, together with the increase in molecular volume with growing particle thickness (at constant σ, see Equation (1)), explain the larger compressibility factors achieved for the fluids with larger L^* (Figure 2). It can be observed that both theoretical EOSs reproduce very well the simulation data for the OHSC fluids with $L^* > 0.3$. At $L^* = 0.3$ and smaller aspect ratios, appreciable differences appear in the immediate vicinity of the liquid crystal transition. Nevertheless, the performance of the relatively simple theories is remarkable, provided that they were developed having as reference fluids of molecules closer to sphericity ($L^* \geq 0.4$).

Figures 4 and 5 show the EOS obtained in our simulation of the different soft oblate Kihara particles described above. Fluids with $L^* = 0.2$ and 0.4 are considered in this case. For soft particles, molecular volume is not well defined, and only the Z versus ρ representation is presented. We recall that the MC simulation of the soft particle fluids was performed at constant pressure ($P^\dagger = 100$), so that the expansion of the fluid follows from sequential heating (see Section 2). Changes in pressure led to qualitatively similar EOSs, with consistent changes in density. It can be observed that both the purely repulsive potential of the OSRS fluid and also the homogeneous attractive well of the KIH fluid lead to a behaviour qualitatively similar to that of the OHSC fluid. The isotropic EOS proceeds smoothly up to relatively high number densities before entering the domain of liquid crystalline behaviour. The liquid crystal transitions in the OSRS and OKIH fluids are similar to their OHSC counterparts, namely I–D_{ho} for $L^* = 0.4$ and I–D_{hd} for $L^* = 0.2$, and occur at not too dissimilar values of Z and ρ^*.

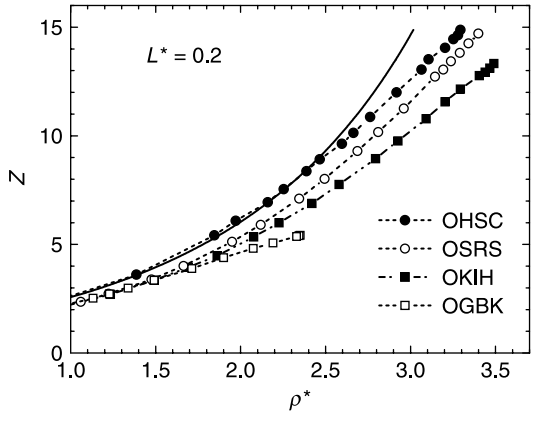

Figure 4. MC compressibility factor $Z = P^*/\rho^*$ versus reduced density $\rho^* = \rho D^3$ representation of the isotropic phase equations of state of the hard and soft discotic potential models considered in this work with $L^* = 0.2$. The theoretical OHSC EOS from [24] is also included for reference (solid line).

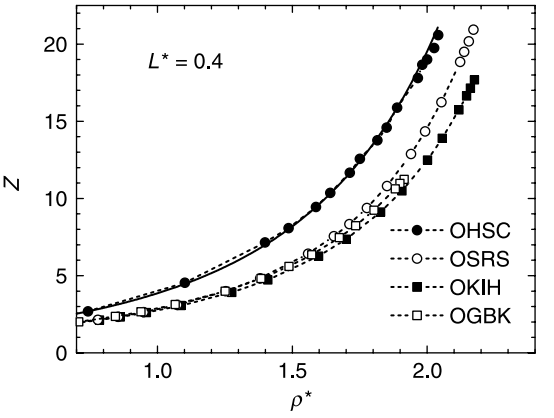

Figure 5. Same as Figure 4 for the hard and soft discotic potential models with $L^* = 0.4$. The theoretical OHSC EOS from [24] is also included for reference (solid line).

In the OGBK model, the specific energetics leads to a significant shift of the liquid phase transition to lower pressures and densities. For the two aspect ratios investigated, $L^* = 0.4$ and $L^* = 0.2$, the OGBK EOS runs at low density close to those of the other soft models. However, the OGBK values of Z, P^* and ρ^* at the transition are appreciably smaller than those for the OHSC, OSRS and OKIH fluids. The comparison of these four models allows us to discern between the steric and the energetic contributions to the free energy responsible for mesogenic behaviour in discotic liquid crystals. Table 1 shows that an appreciable change in internal energy takes place at the isotropic–columnar transitions of the OGBK fluids. The energy discontinuity is much smaller for the OSRS, and even for the OKIH fluids.

A deeper insight into the mesogenic propensity of the Kihara discotic fluids can be grasped from the microscopic structure displayed in the proximity of the liquid crystal transition. Figure 6 shows a selection of radial distribution functions, $g(r)$, for the OHSC, OSRS, OKIH and OGBK fluids with $L^* = 0.2$. For each fluid, the $g(r)$ is shown for the isotropic boundary state of the transition, and at states with densities roughly 85 and 65% of the boundary state density. All distributions show little structure for pair distances greater than the diameter of the molecular core ($r/D > 1$). At $r/D \approx 1$, a differentiated peak is observed, which corresponds to the side-to-side rim contact distance of two parallel discotic spherocylinders. Note that the volume excluded to other particles by a freely rotating spherocylinder in a diluted phase tends to be similar to that of a sphere of its same diameter. Hence, a peak in the pair distribution at $r \approx D$ is indeed expected. Furthermore, it can be observed that this peak persist at low densities. Similarly, a less prominent but also persistent peak is observed at $r/D \approx 0.5 + L^*$, in this case associated to a T-shape-type pair configuration. More interestingly, a marked peak arises in the vicinity of the phase transition

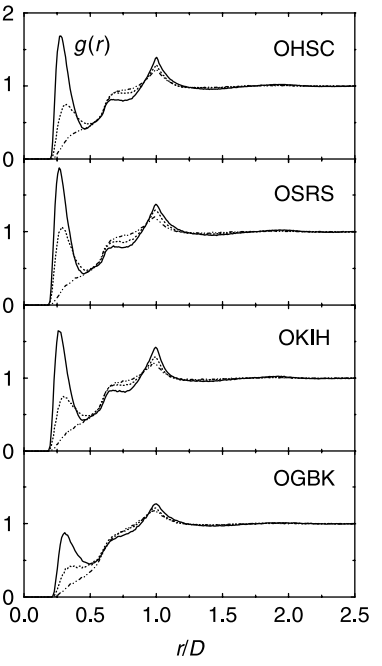

Figure 6. Radial distribution functions, $g(r)$, for the OHSC, OSRS, OKIH and OGBK fluids with $L^* = 0.2$. For each fluid, the $g(r)$ is shown for the isotropic boundary state (solid line) of the transition, and at states with densities roughly 85 and 65% of the boundary state density (dashed and dot-dashed lines, respectively). The pronounced peaks at $r/D \approx L^*$ are indicative of local stacking of the particles.

at $r/D \approx L^*$. This peak is associated with the formation of domains of stacked particles in the isotropic phase. Such stacking domains remain relevant down to densities roughly a factor of 0.7 smaller than that of the boundary state at the liquid crystal transition.

Efficient stacking is observed for all potential energy models, including the purely repulsive OHSC and OSRS fluids. This indicates that stacking can be induced alone from steric interactions induced by the spherocylinder shape of the particles. The specific attractive interactions of the OGBK model further enhance the presence of the stacked domains due to the favourable energetics. In order to appreciate this fact, it should be noted that the distribution functions for the OGBK fluid in Figure 6 correspond to states of smaller density than for the rest of the models. A relevant finding is that for the OGBK fluid, the transition to the columnar phase occurs before extensive short-range stacking can take place in the isotropic phase. This behaviour illustrates how mesoscopic aggregation may be rapidly seeded by local molecular organisation under favourable energetics. On the contrary, the OHSC, OSRS and OKIH fluids allow for a significant degree of short-range organisation before entering the mesoscopic domain.

4. Summary and conclusions

We have presented a simulation study of discotic spherocylinder fluids over a broad range of thickness/diameter ratios $L^* = 0.1–0.5$. In particular, equations of state for fluids with $L^* < 0.3$ are presented for the first time by making use of the shortest distance algorithm reported recently [7]. In addition, four different types of interaction potentials have been considered: a hard (OHSC) and a soft (OSRS) purely repulsive models, a model with a Lennard–Jones attractive potential homogeneously distributed around the molecular core (OKIH) and an attractive potential with an explicit dependence on pair orientation adjusted to favour stacked configurations (OGBK).

We find a remarkable overall agreement between the EOSs obtained by simulation for the OHSC fluid, and the prediction of relatively simple theories. The theoretical EOSs reproduce closely the simulation data for $L^* > 0.3$, whereas at smaller aspect ratios, appreciable differences appear in the immediate vicinity of the liquid crystal transition. The soft OSRS and OKIH fluids follow a similar qualitative behaviour as the OHSC fluid along the isotropic branch, as well as for the location and nature of the columnar transition. For the OGBK model, by contrast, the enhanced stacking interactions lead to a significant anticipation of the liquid crystal transition.

Inspection of the radial distribution function reveals that short-range stacking domains are present in the isotropic phase of the four-model fluids, even at densities significantly lower than that of the columnar transition. A conclusion is that the discotic spherocylinder geometry favours stacking without the need for attractive interactions. The favourable energetics of the OGBK model does not only enhance the appearance of the stacked domains, but it also prompts the columnar transition. On the contrary, the OHSC, OSRS and OKIH fluids allow for a more extensive local stacking in a stable isotropic phase. Such behaviour should be useful to model the potential of local stacking to seed clustering and coagulation processes in colloidal and biomolecular systems. The formation of stacked domains in the isotropic phase should also be of relevance for dynamic energy and charge transfer processes, which often demand directional short-range correlations.

Acknowledgements

Funding is acknowledged from the Regional Government of Andalucia (Projects P06-FQM-01869 and P07-FQM-02600), and from the Ministry of Science and Innovation of Spain (Project ENE2007-68040-C03-01, and the *Juan de la Cierva* fellowship held by A.C.).

Note

1. Email: acuetos@ual.es

References

[1] S. Chandrasekhar, *Columnar, discotic nematic and lamellar liquid crystals: their structures and physical properties*, in *Handbook of Liquid Crystals*, D. Demus, J. Goodby, G.W. Gray, H.-W. Spiess, and V. Vill, eds., Vol. 2B, Wiley-VCH, Weinheim, 1998, pp. 749–780.

[2] R.J. Bushby and O.R. Lozman, *Discotic liquid crystals 25 years on*, Curr. Opin. Coll. Interface Sci. 7 (2002), pp. 343–354.

[3] J. Wu, W. Pisula, and K. Müllen, *Graphenes as potential material for electronics*, Chem. Rev. 107 (2007), pp. 718–747.

[4] Y. Zhao and D.G. Truhlar, *A prototype for graphene material simulation: structures and interaction potentials of coronene dimers*, J. Phys. Chem. C 112 (2008), pp. 4061–4067.

[5] D. Andrienko, V. Marcon, and K. Kremer, *Atomistic simulation of structure and dynamics of columnar phases of hexabenzocoronene derivatives*, J. Chem. Phys. 125 (2006), 124902, pp. 1–8.

[6] P.L. Cristinziano and F. Lelj, *Atomistic simulation of discotic liquid crystals: transition from isotropic to columnar phase example*, J. Chem. Phys. 127 (2007), 134506, 1–13.

[7] A. Cuetos and B. Martínez-Haya, *Columnar phases of discotic spherocylinders*, J. Chem. Phys. 129 (2008), 214706, pp. 1–7.

[8] M.A. Bates and G.R. Luckhurst, *Computer simulation studies of anisotropic systems. XXVI. Monte Carlo investigations of a Gay-Berne discotic at constant pressure*, J. Chem. Phys. 104 (1996), pp. 6696–6709.

[9] E.M. Del Río, A. Galindo, and E. de Miguel, *Density functional theory and simulation of the columnar phase of a system of parallel hard ellipsoids with attractive interactions*, Phys. Rev. E 72 (2005), 051707, pp. 1–12.

[10] M. Wojcik and K.E. Gubbins, *Thermodynamics and structure of hard oblate spherocylinder fluids*, Mol. Phys. 53 (1984), pp. 397–420.

[11] T. Boublik and I. Nezbeda, *P–V–T behaviour of hard body fluids. Theory and experiment*, Coll. Czech. Chem. Commun. 51 (1986), pp. 2301–2432.

[12] W.R. Cooney, S.M. Thompson, and K.E. Gubbins, *Virial-coefficients for the hard oblate spherocylinder fluid*, Mol. Phys. 66 (1989), pp. 1269–1272.

[13] J. Sedlbauer, S. Labik, and A. Malijevsky, *Monte-carlo and integral-equation studies of hard-oblate-spherocylinder fluids*, Phys. Rev. E 49 (1994), pp. 3179–3183.

[14] P. Kadlec, J. Janecek, and T. Boublik, *Systems of oblate molecules. Monte Carlo Study*, Mol. Phys. 98 (2000), pp. 473–479.

[15] M.J. Maeso, J.R. Solana, and J. Amoros, *Equations of state for nonspherical hard-particle fluids*, Mat. Chem. Phys. 33 (1993), pp. 134–138.

[16] B. Mulder, *The excluded volume of hard sphero-zonotopes*, Mol. Phys. 103 (2005), pp. 1411–1424.

[17] F. Gámez, S. Lago, B. Garzón, P.J. Merkling, and C. Vega, *Vapour-liquid equilibrium of fluids composed by oblate molecules*, Mol. Phys. 106 (2008), pp. 1331–1339.

[18] A. Cuetos, B. Martínez-Haya, S. Lago, and L.F. Rull, *Monte Carlo study of liquid crystal phases of hard and soft spherocylinders*, J. Chem. Phys. 117 (2002), pp. 2934–2946.

[19] A. Cuetos, B. Martínez-Haya, S. Lago, and L.F. Rull, *Liquid crystal behavior of the Kihara fluid*, Phys. Rev. E 68 (2003), 011704, pp. 1–4.

[20] B. Martínez-Haya, A. Cuetos, S. Lago, and L.F. Rull, *A novel orientation-dependent potential model for prolate mesogens*, J. Chem. Phys. 122 (2005), 024908, pp. 1–8.

[21] B. Martínez-Haya and A. Cuetos, *Stability of nematic and smectic phases in rod-like mesogens with orientation-dependent attractive interactions*, J. Phys. Chem. B 111 (2007), pp. 8150–8157.

[22] S. Hamad, J.A. Mejías, S. Lago, S. Picaud, and P.N.M. Hoang, *Theoretical study of the adsorption of water on a model soot surface: I. Quantum chemical calculations*, J. Phys. Chem. B 108 (2004), pp. 5405–5409.

[23] S. Picaud, P.N.M. Hoang, S. Hamad, J.A. Mejías, and S. Lago, *Theoretical study of the adsorption of water on a model soot surface: II. Molecular dynamics simulations*, J. Phys. Chem. B 108 (2004), pp. 5410–5415.

[24] C. Barrio and J.R. Solana, *Equation of state for fluid mixtures of hard spheres and heteronuclear hard dumbbells*, J. Chem. Phys. 111 (1999), pp. 4640–4669.

[25] T. Boublik, *3rd virial-coefficient and the hard convex body equation of state*, Mol. Phys. 83 (1994), pp. 1285–1297.